Original Article | Genitourinary Imaging

eISSN 2005-8330
https://doi.org/10.3348/kjr.2021.0212
Korean J Radiol 2021;22(12):1996-2005

Korean Journal of Radiology
KJR

Multidetector CT Characteristics of Fumarate Hydratase-Deficient Renal Cell Carcinoma and Papillary Type II Renal Cell Carcinoma

Ling Yang[1]*, Xue-Ming Li[1]*, Ya-Jun Hu[1], Meng-Ni Zhang[2], Jin Yao[1], Bin Song[1]

Departments of [1]Radiology and [2]Pathology, West China Hospital, Sichuan University, Chengdu, China

Objective: To investigate the multidetector computed tomography (MDCT) features of fumarate hydratase-deficient renal cell carcinoma (FH-deficient RCC) with germline or somatic mutations, and compare them with those of papillary type II RCC (pRCC type II).

Materials and Methods: A total of 24 patients (mean ± standard deviation, 40.4 ± 14.7 years) with pathologically confirmed FH-deficient RCC (15 with germline and 9 with somatic mutations) and 54 patients (58.6 ± 12.6 years) with pRCC type II were enrolled. The MDCT features were retrospectively reviewed and compared between the two entities and mutation subgroups, and were correlated with the clinicopathological findings.

Results: All the lesions were unilateral and single. Compared with pRCC type II, FH-deficient RCC was more prevalent among younger patients (40.4 ± 14.7 vs. 58.6 ± 12.6, $p < 0.001$) and tended to be larger (8.1 ± 4.1 vs. 5.4 ± 3.2, $p = 0.002$). Cystic solid patterns were more common in FH-deficient RCC (20/24 vs. 16/54, $p < 0.001$), with 16 of the 20 (80.0%) cystic solid tumors having showed typical polycystic and thin smooth walls and/or septa, with an eccentric solid component. Lymph node (16/24 vs. 16/54, $p = 0.003$) and distant (11/24 vs. 3/54, $p < 0.001$) metastases were more frequent in FH-deficient RCC. FH-deficient RCC and pRCC type II showed similar attenuation in the unenhanced phase. The attenuation in the corticomedullary phase (CMP) (76.3% ± 25.0% vs. 60.2 ± 23.6, $p = 0.008$) and nephrographic phase (NP) (87.7 ± 20.5, vs. 71.2 ± 23.9, $p = 0.004$), absolute enhancement in CMP (39.0 ± 24.8 vs. 27.1 ± 22.7, $p = 0.001$) and NP (50.5 ± 20.5 vs. 38.2 ± 21.9, $p = 0.001$), and relative enhancement ratio to the renal cortex in CMP (0.35 ± 0.26 vs. 0.24 ± 0.19, $p = 0.001$) and NP (0.43 ± 0.24 vs. 0.29 ± 0.19, $p < 0.001$) were significantly higher in FH-deficient RCC. No significant difference was found between the FH germline and somatic mutation subgroups in any of the parameters.

Conclusion: The MDCT features of FH-deficient RCC were different from those of pRCC type II, whereas there was no statistical difference between the germline and somatic mutation subgroups. A kidney mass with a cystic solid pattern and metastatic tendency, especially in young patients, should be considered for FH-deficient RCC.

Keywords: *Fumarate hydratase; Carcinoma; Renal cell; Papillary; Hereditary leiomyomatosis and renal cell carcinoma*

INTRODUCTION

Fumarate hydratase-deficient renal cell carcinoma (FH-deficient RCC) is a rare subtype of renal cell carcinoma (RCC) with pathologic germline/somatic mutations in the FH gene [1-6]. Lesions with germline mutations are associated

Received: January 2, 2021 **Revised:** June 8, 2021 **Accepted:** July 20, 2021
This study was supported by the Key R & D projects of Sichuan Science and Technology Department (2020YFS0120).
*These authors contributed equally to this work.
Corresponding author: Jin Yao, PhD, Department of Radiology, West China Hospital, Sichuan University, 37# Guoxue Street, Wuhou District, Chengdu, Sichuan 610041, China.
• E-mail: shelleyyao@163.com; and
Bin Song, PhD, Department of Radiology, West China Hospital, Sichuan University, 37# Guoxue Street, Wuhou District, Chengdu, Sichuan 610041, China.
• E-mail: songlab_radiology@163.com

Korean Journal of Radiology
KJR

with hereditary leiomyomatosis and RCC (HLRCC) syndrome, which is an autosomal dominant disorder that predisposes individuals to multiple cutaneous leiomyomas, uterine leiomyomas, and RCC [1,2,6-8]. Clinically, FH-deficient RCC is an aggressive tumor that commonly presents with locally advanced or metastatic disease, even in the setting of a small primary tumor, and with a high rate of progression and mortality [1,2,4,7-10]. Sun et al. [5] found that some patients could benefit from immune checkpoint blockade-based strategies, so timely diagnosis and effective treatment are particularly important.

However, its diagnosis is difficult because of variable and mixed pathological architectures [1,3,5], and it has been misclassified as papillary type II RCC (pRCC type II) when diagnosed via histopathology alone [8,11-13]. Previous studies reported that patients with FH-deficient RCC (germline or somatic) shared remarkable clinical-pathological characteristics with those of HLRCC-associated RCC, which was recognized as a separate entity in the 2016 World Health Organization (WHO) classification; both show characteristics such as younger age at presentation, aggressive clinical behavior, and adverse morphologic features, typically papillary architecture admixed with other growth patterns [1-3]. Recently, some studies have investigated the imaging findings of papillary type II HLRCC-associated renal tumors [12] and FH-deficient RCC [14]; however, they did not clarify the features that could differentiate FH-deficient RCC from pRCC type II, which could help pathologists in making decisions regarding further immunohistochemical staining or even gene sequencing.

To the best of our knowledge, the imaging features of FH-deficient RCC with germline or somatic mutations and their differences from pRCC type II have not been systematically reported. This study aimed to investigate the multidetector computed tomography (MDCT) findings of gene sequencing-confirmed FH-deficient RCC, including an analysis of subgroups of FH germline and somatic mutations, and compare them with pRCC type II.

MATERIALS AND METHODS

Patients

This study was approved by the local Institutional Review Board (IRB No. HX-IRB-AF-16-V4.0), which waived the need for individual consent. From January 2010 to June 2020, 24 patients (mean age ± standard deviation [SD], 40.4 ± 14.7 years; range, 13–71 years) with pathological immunohistochemistry (IHC)-confirmed RCC with FH protein deficiency via punctured or radical specimen were enrolled from 4 hospitals (7 of them were consultation cases from 3 cooperative hospitals); in which 4 cases were retrospectively reviewed and confirmed by IHC from all pRCC cases at our institution before 2017 by a genitourinary pathologist with 20 years of experience. A total of 15 patients (mean age, 40.2 ± 17.3 years, range, 13–71 years) had FH germline mutations and were diagnosed as HLRCC-associated RCC, while the other 9 patients had somatic mutations (mean age, 40.7 ± 9.6 years, range, 26–57 years). The FH gene mutation in all diagnosed FH-deficient RCCs was confirmed by Sanger sequencing [5]. In addition, 54 consecutive patients (mean age 58.6 ± 12.6 years; range, 25–88 years) in our institution with pathologically diagnosed pRCC type II from January 2010 to June 2020 were enrolled as control groups. All patients underwent pre-treatment MDCT examinations.

CT Protocol

All patients underwent plain and double-phase enhanced MDCT examinations. The scan techniques varied somewhat, owing to the retrospective nature of the study. After imaging in the unenhanced phase (UP), 100–150 mL of intravenous contrast media (ominipaque, iopamidol, iopromide) was administered by a power injection at a rate of 3 mL/s, with a dose of approximately 2 mL/kg. Subsequently, corticomedullary phase (CMP) and nephrographic phase (NP) scans were initiated at 20–30 seconds and 60–80 seconds after the initiation of the injection, respectively. In general, the examinations were performed using a spiral technique with 2–5 mm collimation and 2–5 mm reconstruction intervals. Patients were scanned using several MDCT scanners (Ingenuity, Brilliance 64, Philips Healthcare; SOMATOM Definition AS+/Flash and Sensation 16, Siemens Medical Solutions; Revolution CT, GE Healthcare), with 120 kV voltage and 120–210 mA current.

Imaging Analysis

The images were reviewed by two radiologists with 5 and 15 years of experience in abdominal imaging, respectively; both radiologists were aware of the presence of renal tumor but were blinded to the clinical and histopathological results. The lesions were evaluated for laterality, single or multiple, maximal diameter, location (left or right), growth pattern (exophytic or endophytic), solid or cystic solid

 https://doi.org/10.3348/kjr.2021.0212

(predominantly solid or predominantly cystic), calcification, hemorrhage, necrosis, perirenal fat invasion, renal sinus invasion, renal venous thrombus, lymph node, and distant metastasis. The CT values of the lesions and normal renal cortex (ipsilateral or contralateral) were measured on UP, CMP, and NP at the same level, with slice thickness reconstructed to 5 mm. Each radiologist placed two regions of interest (approximately 0.5–1 cm^2) at the solid part of the tumor and renal cortex.

Endophytic and exophytic growth was defined as the main body of the tumor inside or outside the outline of the kidney, respectively. Predominantly solid and cystic patterns were defined as cystic proportions of < 50% or > 50%. Perirenal fat invasion was characterized as a tumor that had broken through the renal capsule, and renal sinus invasion was characterized as a tumor that had invaded the renal sinus adipose space. Necrosis was defined as an unenhanced low-density area with an ambiguous boundary in the solid part, and cystic area as an unenhanced water density area with a clear boundary around or inside the solid part. When there was a difference between the investigators' opinions, a consensus was reached through discussion or consultation with another senior genitourinary radiologist with more than 15 years of experience. The final unenhanced and enhanced CT values of the lesions and normal renal cortex in different phases were calculated by averaging the values measured by the two radiologists. The absolute enhancement value of the tumor and renal cortex in CMP/NP was calculated by subtracting the CT value in CMP/NP and UP, and the relative enhancement ratio of the lesion in CMP and NP was calculated using the following formula: the absolute enhancement value of the lesions / the absolute enhancement value of the renal cortex.

Statistical Analysis

All statistical analyses were performed using IBM SPSS version 21.0. (IBM Corp., Armonk, NY, USA). Continuous and categorical variables were expressed as mean ± SD or percentage, respectively, and they were compared between the groups using the unpaired student *t* test or chi-square test. Statistical significance was defined as a two-tailed *p* value < 0.05.

RESULTS

Pathological and Clinical Characteristics of FH-Deficient RCC

Microscopically, the lesions showed multiple microstructures, such as papillary, nested, tubular, tubulocystic, and cystic patterns. The International Society of Urological Pathology (ISUP)/WHO grade was 2 in 1 patient, 3 in 20 patients, and 4 in 3 patients. Among the seven female patients, one had a germline mutation and a history of familial uterine leiomyomas, and three had uterine leiomyomas and somatic mutations. In addition, only one male patient was documented to have typical cutaneous leiomyomas, and he had an FH somatic mutation.

Nineteen patients showed symptoms, such as hematuria (10/24, 41.7%), low back pain (8/24, 33.3%), and weakness (1/24, 4.2%), at the time of initial diagnosis, while they were found on routine medical examination in others. In addition, none of the patients had a family history of RCC. A total of 4 patients with lymph node and distant metastasis at diagnosis were treated with radio-, interventional, or targeted therapy, in which 2 patients were stable for 6 and 10 months, respectively, and the other 2 patients progressed in 2 and 13 months, respectively. The remaining 20 patients underwent surgery and adjuvant therapy when there was initial metastasis or postoperative progression. Of these patients, 2 died 10 and 12 months later, respectively, without timely adjuvant therapy, before 2017; 4 lived without recurrence from 6 to 90 months without any adjuvant therapy; 10 progressed within 2 to 19 months after surgical therapy; 3 were unevaluable due to short follow-up time; and one was lost to follow-up.

Imaging Characteristics of FH-Deficient RCC and pRCC Type II

The main imaging characteristics of the two entities and subgroups of FH-deficient RCC are summarized in Tables 1 and 2.

All the lesions involved were unilateral and single. Both FH-deficient RCC and pRCC type II showed similar distributions in terms of sex, location (left/right), and growth pattern (exophytic/endophytic). The age was significantly lower in patients with FH-deficient RCC ($p < 0.001$), with the number of patients below 40 years of age being 13 (13/24, 54.2%) in FH-deficient RCC, but only 3 (3/54, 5.6%) in the pRCC type II group. Compared with pRCC type II, FH-deficient RCC predisposes patients to

https://doi.org/10.3348/kjr.2021.0212

Korean Journal of Radiology
KJR

Table 1. Comparison between FH-Deficient RCC and pRCC Type II

Characteristics	FH-Deficient RCC (n = 24)	pRCC Type II (n = 54)	*P*
Age, year	40.4 ± 14.7 (13–71)	58.6 ± 12.6 (25–88)	< 0.001
Female	7 (29.2)	10 (18.2)	0.787
Diameter, cm	8.1 ± 4.1 (3.0–19.8)	5.4 ± 3.2 (1.2–14.8)	0.002
Location in the left kidney	16 (66.7)	29 (53.7)	0.329
Exophytic	15 (62.5)	32 (59.3)	1.000
Solid and cystic pattern			< 0.001
Solid	4 (16.6)	38 (70.4)	
Predominantly cystic	10 (41.7)	3 (5.5)	
Predominantly solid	10 (41.7)	13 (24.1)	
Calcification	6 (25.0)	12 (22.2)	1.000
Hemorrhage	3 (12.5)	4 (7.4)	0.670
Necrosis	15 (62.5)	25 (46.3)	0.225
Perirenal fat invasion	7 (29.2)	11 (20.4)	0.561
Renal sinus invasion	9 (37.5)	15 (27.8)	0.432
Renal venous thrombus	4 (16.7)	5 (9.3)	0.445
Lymph node	16 (66.7)	16 (29.6)	0.003
Distant metastasis	11 (45.8)	3 (5.6)	< 0.001
Unenhanced attenuation, HU	37.2 ± 8.32 (29.0–70.0)	38.4 ± 11.0 (19.7–74.0)	0.638
Attenuation in CMP, HU	76.3 ± 25.0 (45.2–135.3)	60.2 ± 23.6 (30.0–123.3)	0.008
Attenuation in NP, HU	87.7 ± 20.5 (58.3–132.0)	71.2 ± 23.9 (32.0–128.0)	0.004
Absolute enhancement in CMP, HU	39.0 ± 24.8	27.1 ± 22.7	0.001
Absolute enhancement in NP, HU	50.5 ± 20.5	38.2 ± 21.9	0.001
Relative enhanced ratio in CMP	0.35 ± 0.26	0.24 ± 0.19	0.001
Relative enhanced ratio in NP	0.43 ± 0.24	0.29 ± 0.19	< 0.001
Ratio of unenhanced value	1.11 ± 0.26	1.18 ± 0.26	0.107

Data are mean ± standard deviation with or without range in parentheses or raw number with percentages in parentheses. CMP = corticomedullary phase, FH-deficient RCC = fumarate hydratase-deficient renal cell carcinoma, HU = Hounsfield unit, NP = nephrographic phase, pRCC type II = papillary type II renal cell carcinoma

larger tumors (p = 0.002).

In the FH-deficient RCC group, four of the lesions (4/24, 16.7%) were solid (Fig. 1), showed germline mutations, and mainly demonstrated papillary or tubular pathological morphology, with two being mixed with solid or adenoid pattern. A total of 10 (10/24, 41.7%) lesions were predominantly solid (Fig. 2), and mainly showed papillary, tubular, or adenoid pattern, with some cases mixed with solid or nested pattern; the other 10 (10/24, 41.7%) lesions were predominantly cystic (Fig. 3) and mainly showed papillary or tubular pattern, with some cases mixed with cystic or adenoid pattern. Among all the cystic solid tumors, the solid part was eccentric and adjacent to the renal sinus, and the cystic part was inclined to grow, deviating from the renal sinus. In addition, 16 (16/20, 80.0%) cystic solid lesions showed a polycystic pattern with a thin, smooth wall and/or septum. In the pRCC type II group, only 16 (16/54, 29.6%) lesions showed a cystic solid pattern, of which 13 (13/54, 24.1%) were predominantly solid and 3 (3/54, 5.5%) were predominantly cystic. Six patients (6/16, 37.5%) had a thin septum. In total, the distributions of solid and cystic solid patterns were significantly different between the two entities (p < 0.001).

Compared with the pRCC type II group, there was no statistical difference in the distribution of calcification, hemorrhage, necrosis, perirenal fat invasion, renal venous thrombus, and renal sinus invasion between the two entities. Lymph node metastasis was found in 16 FH-deficient RCC patients (3 solid and 13 cystic solid), and 11 of them (2 solid, 9 cystic solid) showed distant metastasis in the bone, lung, adrenal gland, liver, or pleura. A total of 16 patients with pRCC type II (8 solid and 8 cystic solid) had lymph node metastasis, and 3 (1 solid and 2 cystic solid) had distant metastases in the bone and adrenal gland. Both lymph node and distant metastases were more frequent in the FH group (p = 0.003 and p < 0.001, respectively).

The mean double-phase attenuation of both entities in

 https://doi.org/10.3348/kjr.2021.0212

Table 2. Comparison between FH-Deficient RCC Subgroups

Characteristics	Somatic FH-Deficient RCC (n = 9)	Germline FH-Deficient RCC (n = 15)	*P*
Age, year	40.7 ± 9.6 (26–57)	40.2 ±17.3 (13–71)	0.942
Female	4 (44.4)	3 (20)	0.417
Diameter, cm	7.5 ± 3.4 (3.0–13.2)	8.5 ± 4.5 (3.8–19.8)	0.592
Location in the left kidney	5 (55.6)	11 (73.3)	0.655
Exophytic	7 (77.8)	9 (60.0)	0.446
Solid and cystic pattern			0.213
Solid	0	4 (26.7)	
Predominantly cystic	5 (55.6)	5 (33.3)	
Predominantly solid	4 (44.4)	6 (40.0)	
Calcification	2 (22.2)	4 (26.6)	1.000
Hemorrhage	0	3 (20.0)	0.266
Necrosis	5 (55.6)	10 (66.7)	0.913
Perirenal fat invasion	1 (11.1)	6 (40.0)	0.297
Renal sinus invasion	2 (22.2)	7 (46.7)	0.446
Renal venous thrombus	0	4 (26.6)	0.259
Lymph node	6 (66.6)	10 (66.7)	1.000
Distant metastasis	4 (44.4)	7 (46.7)	1.000
Unenhanced attenuation, HU	35.6 ± 4.79 (29.0–40.0)	38.2 ± 9.89 (29.0–70.0)	0.468
Attenuation in CMP, HU	76.8 ± 28.3 (45.2–135.3)	76.0 ± 23.9 (49.0–132.9)	0.946
Attenuation in NP, HU	88.5 ± 25.6 (58.3–131.6)	87.2 ± 17.6 (62.0–116.0)	0.881
Absolute enhancement in CMP, HU	22.2 ± 21.2	25.1 ± 20.4	0.758
Absolute enhancement in NP, HU	28.8 ± 21.2	36.2 ± 15.6	0.336
Relative enhanced ratio in CMP	0.18 ± 0.15	0.22 ± 0.15	0.459
Relative enhanced ratio in NP	0.20 ± 0.11	0.28 ± 0.12	0.096
Ratio of unenhanced value	1.31 ± 0.20	1.13 ± 0.23	0.065

Data are mean ± standard deviation with or without range in parentheses or raw number with percentages in parentheses. CMP = corticomedullary phase, FH-deficient RCC = fumarate hydratase-deficient renal cell carcinoma, HU = Hounsfield unit, NP = nephrographic phase

UP, CMP, and NP is shown in Figure 4. The attenuation of lesions in CMP and NP (p = 0.008 and 0.004, respectively), absolute enhancement in CMP and NP (all p = 0.001), and relative enhancement ratio to the cortex in CMP and NP (p = 0.001 and p < 0.001, respectively) in the FH group was significantly higher than that in the pRCC type II group. The unenhanced attenuation of lesions was higher than that of the renal cortex in both entities, while there was no statistical difference in the lesion attenuation and its ratio to the renal cortex in UP.

None of these clinical and imaging parameters were statistically different between the two mutation subgroups of FH-deficient RCC (Table 2).

DISCUSSION

HLRCC-associated RCC is an extremely rare and aggressive subtype of RCC found in approximately 15%–34% of reported HLRCC-affected families worldwide, and germline mutations in the FH gene (1q42.3–q43) have been reported to cause the syndrome [2,7,10,15]. FH-deficient RCC has been proposed as a broader disease as it contains both germline and somatic mutation subtypes [2]. Multiple, and sometimes mixed, architectures have been observed in FH-deficient RCC, such as papillary, tubulopapillary, tubulocystic, tubular, cribriform, sarcomatoid, and rhabdoid [1-4,8], with most of our cases showing predominantly papillary or tubular patterns. The diagnosis of FH-deficient RCC based on architectural patterns is difficult and it may be confused with pRCC type II when diagnosed only through microscopic examination. The diagnosis must be further confirmed by IHC, specifically via positivity for S-(2-succinyl) cysteine (2SC) and negativity for FH, CK7, and AMACR expression [1,4,7,8], or even gene sequencing. High rates of aggressive behavior, relapse, and mortality have highlighted the importance of recognition and specific treatment for this entity as soon as possible [1-3]. Radiologists, who might confront this type of tumor first

https://doi.org/10.3348/kjr.2021.0212

Korean Journal of Radiology
KJR

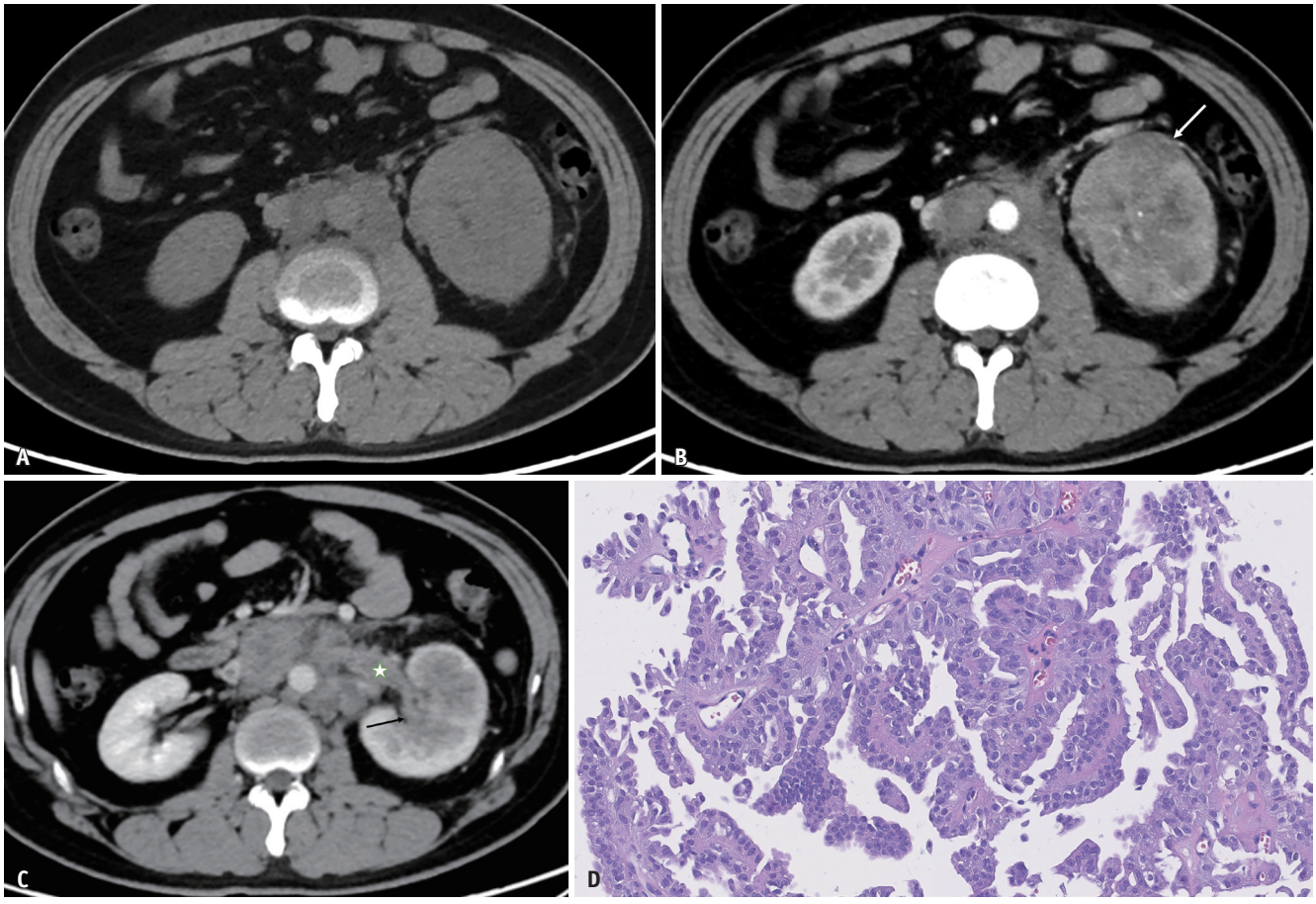

Fig. 1. A 30-year-old male with solid fumarate hydratase-deficient renal cell carcinoma with germline mutation in the left kidney. A-D. CT images in the unenhanced **(A)**, corticomedullary **(B)**, and nephrographic **(C)** phases show an indistinct left renal mass with moderate enhancement. Enhanced axial images show simultaneous perirenal fat invasion (white arrow), renal sinus invasion (black arrow), renal venous tumor thrombus (star), and lymph node metastasis **(B, C)**. Histopathologic photograph showing a papillary growth pattern (hematoxylin and eosin stain, x 200) **(D)**.

and evaluate the overall tumor characteristics, must be familiar with the clinical and specific imaging features to alert pathologists to perform relevant IHC or genetic examinations in cases with suspicious imaging features.

A previous report from Europe found that FH-deficient RCC was associated with HLRCC syndrome in approximately 35.0% of patients [2]. In our study, only one patient with a germline mutation had familiar uterine leiomyomas, while four patients with somatic mutations showed HLRCC syndrome-associated symptoms, which may indicate that these HLRCC syndrome-associated symptoms could also be found in sporadic cases. Previous studies have found that HLRCC-associated RCC has a high rate of metastasis, even when the tumor is small or at an early stage, with a high fatality rate [8,9,16]. The proportion of patients with distant metastasis was higher in our study (45.8% vs. 19.0%) than in the study by Trpkov et al. [2], while that of lymph node metastasis was similar (66.7% vs. 52.0%). The mortality rate was lower (8.3% vs. 39.0%), but the progression rate was higher (41.7% vs. 26.0%), which may be due to differences in race, therapy, and follow-up time.

Pathologically, FH-deficient RCC may present with a prominent tubulocystic and microcystic growth pattern, or even an entirely cystic pattern [2,8]. The Krebs cycle enzyme, FH, is a human tumor suppressor whose inactivation is associated with the development of leiomyoma, renal cysts, and tumors [17]. FH1 loss induces early renal cyst formation, dysplastic changes in cystic epithelium, and solid tumors arising from cyst walls, which may suggest that cystic change is the early stage of carcinogenesis [17], and it helps explain the cystic solid pattern of FH-deficient RCC. Previous studies have also proposed that cystic formation might be caused by a tumor originating from the epithelium of the proximal convoluted tubule, which grows in a cystic pattern [18,19]. There was no statistical difference in the distribution of solid and cystic solid patterns between the

 https://doi.org/10.3348/kjr.2021.0212

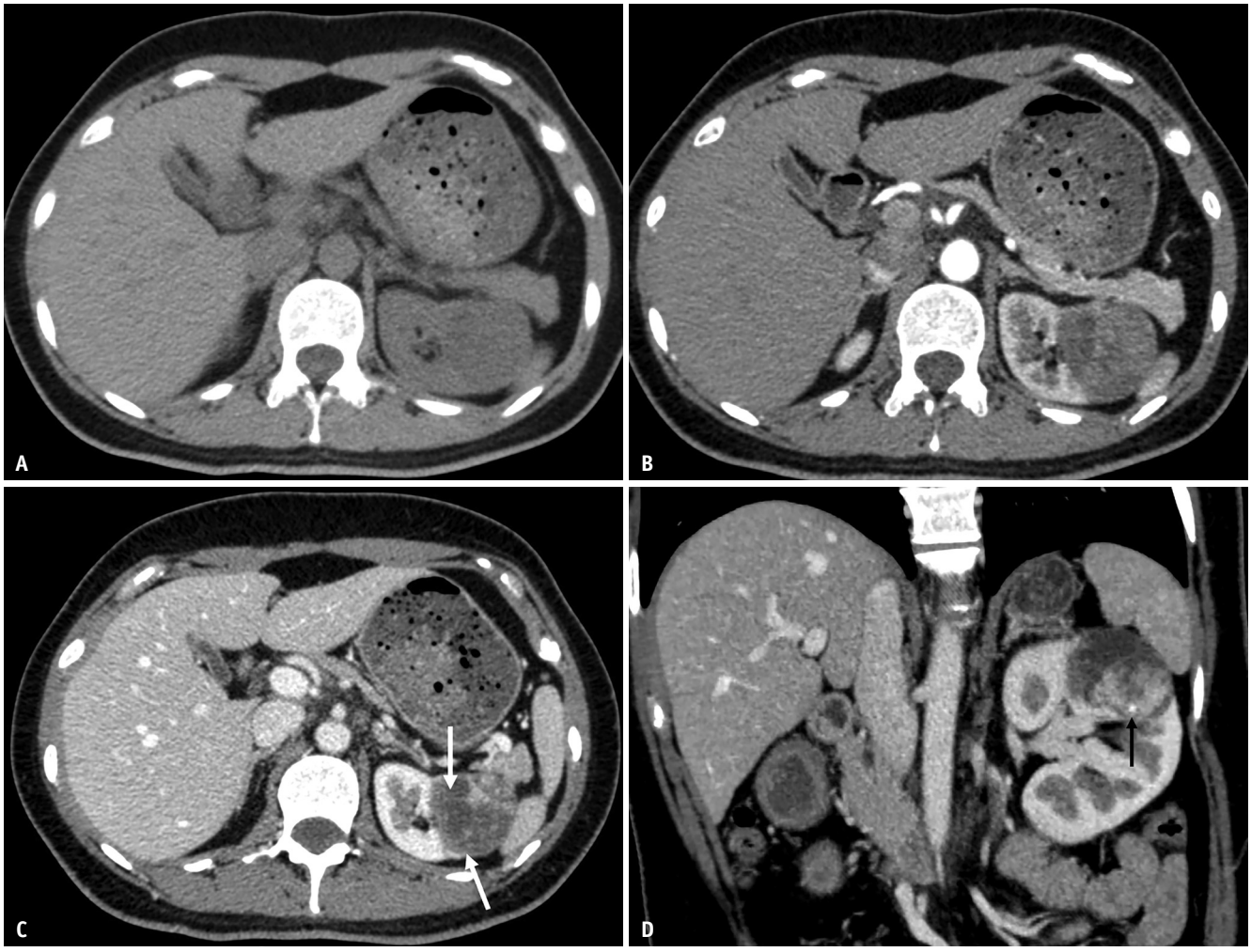

Fig. 2. A 37-year-old female with predominantly solid fumarate hydratase-deficient renal cell carcinoma with somatic mutation in the left kidney. A-D. An unenhanced CT image **(A)** shows a soft tissue mass mixed with a low-density area. Corticomedullary **(B)** and nephrographic **(C, D)** phase CT images show the eccentric location of the solid portion with a thin septum (white arrows) and calcification (black arrow).

germline and somatic mutation groups in our cases, which may suggest that a cystic solid pattern is likely to occur as long as FH-deficiency exists in the tumor.

With a cystic solid pattern, FH-deficient RCC should be differentiated from other renal tumors with similar characteristics. The mixed cystic solid (83.4%) pattern was more commonly found in FH-deficient RCC than in pRCC type II (29.6%) in our study, as well as other common subtypes of renal tumors reported, such as clear cell RCC (22.9%–54.1%), pRCC type I (23.0%–36.4%), and chromophobe RCC (12.5%–21.9%) [12,20,21]. Polycystic (80.0%) change with thin, smooth wall and/or septum could be considered a characteristic feature of FH-deficient RCC in our study, which could also be seen in previously reported papillary type II HLRCC-associated renal tumors but without systematic exposition [12,14]. Although clear cell RCC was the most common cystic solid RCC, its enhancement peaked in CMP, which was significantly different from that of FH-deficient RCC [22]. Compared with the CT appearance of multilocular cystic RCC (MCRCC) with a measurable enhanced thick or irregular wall and septa [23], the wall and septa of FH-deficient RCC are thin and always unmeasurable. In addition, MCRCC has been shown to have a highly innocuous natural history with a low grade and absence of metastasis [24], which also differs from our cases. Typically, the size of tubulocystic RCCs (TCRCC) is small, and approximately 40.0% of them are smaller than 2 cm [18], unlike the FH-deficient RCC observed in our cases. As reported in the literature, cystic pattern and rim-like or egg-shell calcification are common in Xp11.2/TFE RCC [25-27]. However, the probability of a polycystic shape was higher, and typical calcification was relatively rare in

https://doi.org/10.3348/kjr.2021.0212

Korean Journal of Radiology
KJR

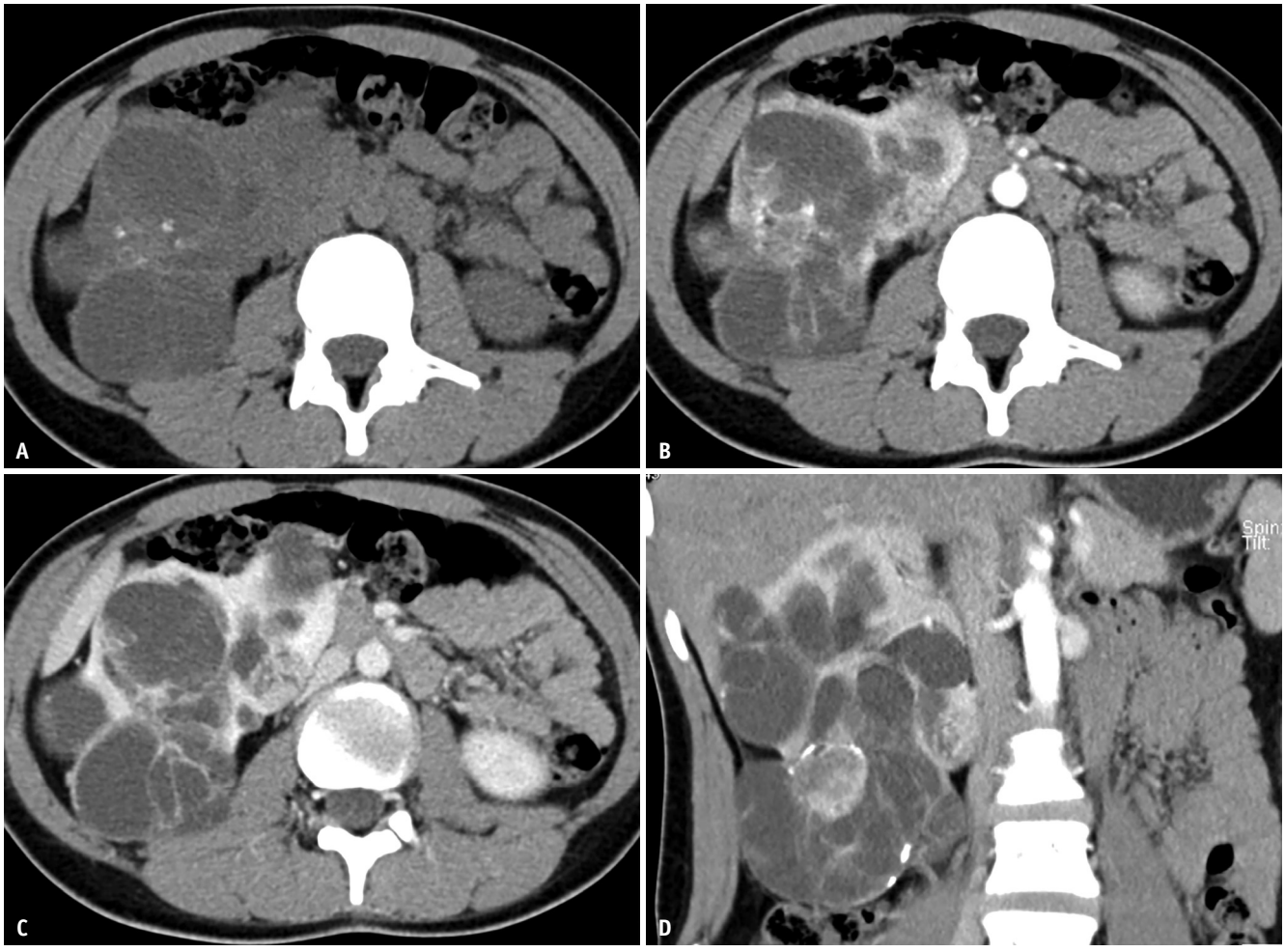

Fig. 3. A 13-year-old girl with predominantly cystic fumarate hydratase-deficient renal cell carcinoma with germline mutation in the right kidney. A-D. An unenhanced CT image **(A)** shows multiple cysts and calcifications. Corticomedullary **(B)** and nephrographic **(C, D)** phase CT images show the eccentric location of the solid portion.

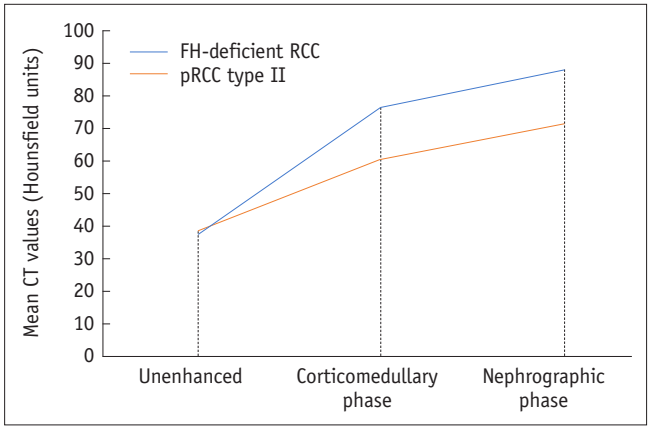

Fig. 4. Mean double-phase attenuation curves for FH-deficient RCC and pRCC type II. FH-deficient RCC = fumarate hydratase-deficient renal cell carcinoma, pRCC type II = papillary type II renal cell carcinoma

FH-deficient RCC.

Similar to pRCC type II, FH-deficient RCC demonstrated progressive enhancement, which peaked in the NP. However, the absolute enhancement and relative enhancement ratios in CMP and NP of FH-deficient RCC were higher than those of pRCC type II. This may be because the most common histopathological characteristic of FH-deficient RCC is papillary, although some are mixed with other forms. Moreover, FH-deficient RCC was susceptible to involvement in younger patients and showed larger size, and the rates of lymph node and distant metastasis were higher in FH-deficient RCC than in pRCC type II in our study, and among other reported subtypes of RCC [12,14,20-24,26].

Due to the high rate of metastasis and lethality of FH-deficient RCC, some authors have suggested that it should be aggressively evaluated and surgically removed [7], and might benefit from systemic therapy [1] and immunotherapy

https://doi.org/10.3348/kjr.2021.0212

[5]. However, high-level evidence regarding optimal and effective management is insufficient because of the limited time until the proposition of this disease [1]. In our study, most patients received targeted therapy after surgery when there was initial metastasis, combined therapy when surgery could not be performed, and close follow-up, especially after 2017. This has achieved certain positive effects compared with previous studies on mortality rate [2], and proved that constantly updating knowledge from clinical, pathological, and radiological aspects can benefit patients in clinical treatment.

There are some limitations to our study. First, 2SC immunostaining was missed because the antibody was not yet commercially available [4]. Second, although the same slice thickness had been reconstructed and corrected with the enhancement of the renal cortex, the variety of scanners used may have impacted the measurement of CT values, which was difficult to avoid, and sometimes, it was not easy to distinguish between cystic degeneration and necrosis. Finally, the limited sample size and short follow-up period may have cause inaccurate statistical results and prognosis judgment. However, this was still the largest sample of FH-deficient RCC that considered germline/somatic mutation and compared with pRCC type II in imaging findings for the first time.

In conclusion, the MDCT features of FH-deficient RCC were different from those of pRCC type II, whereas there was no statistical difference between the germline and somatic mutation subgroups. A kidney mass with a cystic solid pattern and metastatic tendency, especially in young patients, should be considered suspicious for FH-deficient RCC.

Conflicts of Interest

The authors have no potential conflicts of interest to disclose.

Acknowledgments

The authors are grateful for the support of the tissue specimens and the image data from the cooperative units (Sichuan Provincial people's Hospital, China, Zigong fourth people's Hospital, Sichuan, China and Chinese PLA General Hospital [301 Hospital]).

Author Contributions

Conceptualization: all authors. Data curation: Ling Yang, Xue-Ming Li, Ya-Jun Hu. Formal analysis: Ling Yang, Xue-Ming Li, Jin Yao, Bin Song. Investigation: Meng-Ni Zhang. Methodology: Ya-Jun Hu. Supervision: Jin Yao, Bin Song. Wright—original draft: Ling Yang, Xue-Ming Li, Jin Yao, Bin Song. Writing—review & editing: Jin Yao, Bin Song.

ORCID iDs

Ling Yang
https://orcid.org/0000-0001-5674-7347
Xue-Ming Li
https://orcid.org/0000-0002-6165-453X
Ya-Jun Hu
https://orcid.org/0000-0002-3777-0389
Meng-Ni Zhang
https://orcid.org/0000-0002-2906-5161
Jin Yao
https://orcid.org/0000-0003-3028-9370
Bin Song
https://orcid.org/0000-0002-7269-2101

REFERENCES

1. Lau HD, Chan E, Fan AC, Kunder CA, Williamson SR, Zhou M, et al. A clinicopathologic and molecular analysis of fumarate hydratase-deficient renal cell carcinoma in 32 patients. *Am J Surg Pathol* 2020;44:98-110
2. Trpkov K, Hes O, Agaimy A, Bonert M, Martinek P, Magi-Galluzzi C, et al. Fumarate hydratase–deficient renal cell carcinoma is strongly correlated with fumarate hydratase mutation and hereditary leiomyomatosis and renal cell carcinoma syndrome. *Am J Surg Pathol* 2016;40:865-875
3. Smith SC, Trpkov K, Chen YB, Mehra R, Sirohi D, Ohe C, et al. Tubulocystic carcinoma of the kidney with poorly differentiated foci: a frequent morphologic pattern of fumarate hydratase-deficient renal cell carcinoma. *Am J Surg Pathol* 2016;40:1457-1472
4. Pan X, Zhang M, Yao J, Zeng H, Nie L, Gong J, et al. Fumaratehydratase-deficient renal cell carcinoma: a clinicopathological and molecular study of 13 cases. *J Clin Pathol* 2019;72:748-754
5. Sun G, Zhang X, Liang J, Pan X, Zhu S, Liu Z, et al. Integrated molecular characterization of fumarate hydratase-deficient renal cell carcinoma. *Clin Cancer Res* 2021;27:1734-1743
6. Gupta S, Erickson LA. Fumarate hydratase-deficient renal cell carcinoma. *Mayo Clin Proc* 2020;95:619-621
7. Patel VM, Handler MZ, Schwartz RA, Lambert WC. Hereditary leiomyomatosis and renal cell cancer syndrome: an update and review. *J Am Acad Dermatol* 2017;77:149-158
8. Skala SL, Dhanasekaran SM, Mehra R. Hereditary leiomyomatosis and renal cell carcinoma syndrome (HLRCC): a contemporary review and practical discussion of the differential diagnosis for HLRCC-associated renal cell

https://doi.org/10.3348/kjr.2021.0212

carcinoma. *Arch Pathol Lab Med* 2018;142:1202-1215
9. Grubb RL 3rd, Franks ME, Toro J, Middelton L, Choyke L, Fowler S, et al. Hereditary leiomyomatosis and renal cell cancer: a syndrome associated with an aggressive form of inherited renal cancer. *J Urol* 2007;177:2074-2079
10. Refae MA, Wong N, Patenaude F, Bégin LR, Foulkes WD. Hereditary leiomyomatosis and renal cell cancer: an unusual and aggressive form of hereditary renal carcinoma. *Nat Clin Pract Oncol* 2007;4:256-261
11. Freifeld Y, Ananthakrishnan L, Margulis V. Imaging for screening and surveillance of patients with hereditary forms of renal cell carcinoma. *Curr Urol Rep* 2018;19:82
12. Paschall AK, Nikpanah M, Farhadi F, Jones EC, Wakim PG, Dwyer AJ, et al. Hereditary leiomyomatosis and renal cell carcinoma (HLRCC) syndrome: spectrum of imaging findings. *Clin Imaging* 2020;68:14-19
13. Ooi A. Advances in hereditary leiomyomatosis and renal cell carcinoma (HLRCC) research. *Semin Cancer Biol* 2020;61:158-166
14. Nikolovski I, Carlo MI, Chen YB, Vargas HA. Imaging features of fumarate hydratase-deficient renal cell carcinomas: a retrospective study. *Cancer Imaging* 2021;21:24
15. Gardie B, Remenieras A, Kattygnarath D, Bombled J, Lefèvre S, Perrier-Trudova V, et al. Novel FH mutations in families with hereditary leiomyomatosis and renal cell cancer (HLRCC) and patients with isolated type 2 papillary renal cell carcinoma. *J Med Genet* 2011;48:226-234
16. Sudarshan S, Pinto PA, Neckers L, Linehan WM. Mechanisms of disease: hereditary leiomyomatosis and renal cell cancer--a distinct form of hereditary kidney cancer. *Nat Clin Pract Urol* 2007;4:104-110
17. Adam J, Hatipoglu E, O'Flaherty L, Ternette N, Sahgal N, Lockstone H, et al. Renal cyst formation in Fh1-deficient mice is independent of the Hif/Phd pathway: roles for fumarate in KEAP1 succination and Nrf2 signaling. *Cancer Cell* 2011;20:524-537
18. Honda Y, Nakamura Y, Goto K, Terada H, Sentani K, Yasui W, et al. Tubulocystic renal cell carcinoma: a review of literature focused on radiological findings for differential diagnosis. *Abdom Radiol (NY)* 2018;43:1540-1545
19. Zhang J, Liu B, Song N, Hua L, Wang Z, Gu M, et al. Diagnosis and treatment of cystic renal cell carcinoma. *World J Surg Oncol* 2013;11:158
20. Ching BC, Tan HS, Tan PH, Toh CK, Kanesvaran R, Ng QS, et al. Differential radiologic characteristics of renal tumours on multiphasic computed tomography. *Singapore Med J* 2017;58:262-266
21. Fu W, Huang G, Moloo Z, Girgis S, Patel VH, Low G. Multimodality imaging characteristics of the common renal cell carcinoma subtypes: an analysis of 544 pathologically proven tumors. *J Clin Imaging Sci* 2016;6:50
22. Moldovanu CG, Petresc B, Lebovici A, Tamas-Szora A, Suciu M, Crisan N, et al. Differentiation of clear cell renal cell carcinoma from other renal cell carcinoma subtypes and benign oncocytoma using quantitative MDCT enhancement parameters. *Medicina (Kaunas)* 2020;56:569
23. Palmeiro MM, Niza JL, Loureiro AL, Conceição e Silva JP. Unusual renal tumour: multilocular cystic renal cell carcinoma. *BMJ Case Rep* 2016;2016:bcr2016214386
24. Campbell N, Rosenkrantz AB, Pedrosa I. MRI phenotype in renal cancer: is it clinically relevant? *Top Magn Reson Imaging* 2014;23:95-115
25. Weibl P, Hora M, Kollarik B, Kalusova K, Pitra T, Remzi M, et al. A practical guide and decision-making protocol for the management of complex renal cystic masses. *Arab J Urol* 2017;15:115-122
26. Woo S, Kim SY, Lee MS, Moon KC, Kim SH, Cho JY, et al. MDCT findings of renal cell carcinoma associated with Xp11.2 translocation and TFE3 gene fusion and papillary renal cell carcinoma. *AJR Am J Roentgenol* 2015;204:542-549
27. Liang W, Xu S. Xp11.2 translocation renal cell carcinoma with egg-shell calcification mimicking a benign renal tumour: a case report. *Oncol Lett* 2015;10:3191-3194

 https://doi.org/10.3348/kjr.2021.0212